International Journal of Fluid Machinery and Systems
Vol. 2, No. 1, January-March 2009

Original Paper

Prediction of Wear Depth Distribution by Slurry on a Pump Impeller

Kenichi Sugiyama[1], Hiroshi Nagasaka[2], Takeshi Enomoto[2] and Shuji Hattori[3]

[1]Material Laboratoty, Ebara Research Co., LTD
2-1 Honfujisawa, 4, Fujisawa 251-8502, Japan
[2] Manufacturing Process Development Center, Ebara Corporation
11-1, Haneda Asahi-cho, Ohta-ku, Tokyo 144-8510, Japan
[3]Department of Mechanical Engineering, Fukui University
9-1 Bunkyo 3, Fukui 910-8507, Japan

Abstract

Slurry wear with sand particles in rivers is a serious problem for pump operation. Therefore, a technique to predict wear volume loss is required for selecting wear resistant materials and determining specifications for the maintenance period. This paper reports a method for predicting the wear depth distribution on the blade of an impeller. Slurry wear tests of an aluminum pump impeller were conducted. Prediction results of wear depth distribution approximately correspond with the results of slurry wear tests. This technique is useful for industrial application.

Keywords: Pump, Impeller, Numerical analysis, Slurry wear, Life prediction

1. Introduction

Pumps and other fluid machines used in river water containing a large volume of sand are confronted with slurry wear on their materials. This wear is caused by sand in the fluid repeatedly impacting on the material surfaces; such wear results in serious problems. Pump impellers, in particular, are one of the components significantly subject to slurry wear since flow velocity is high within them. Therefore, a technique for predicting the slurry wear depth distribution on impellers is essential for material selection and maintenance.

Since there are many parameters, including the impact angle and velocity of particles, that affect slurry wear, its mechanism is complex. Accordingly, though there have been several study reports on slurry wear evaluation for impeller blades [1], [2], [3], studies of quantitative wear depth distribution on the entire flow channel wall of impellers have not been reported.

We have conducted basic study on the prediction of slurry wear depth for metal materials used in pumps, such as stainless steel, aluminum, and copper [4-5]. The study has provided a prediction method for wear depth by slurry considering the influence of impact velocity, angle, concentration, and size distribution of particles. However, this method has only been applied to the prediction of wear depth distribution on specimens using a slurry jet test apparatus.

This paper aims to extend the method to the prediction of wear depth distribution on impellers. For this purpose, we have conducted a slurry wear test on the impeller of an actual pump and compared the wear depth distribution after the test with the results from the prediction.

2. Test method

2.1 Test Apparatus and Material

Figure 1 shows the schematic drawing of the slurry jet test apparatus employed for obtaining basic data from the aluminum alloy (JIS A5056) used in the tested impeller. In the past, this test apparatus was used to perform the test for aluminum (A1070BD-F), copper (C1020), martensitic stainless cast steel (SCS6), iron (FC250), and austenitic stainless steel (SUS304). However, since the impeller material, A5056, was not yet tested, a slurry jet test for the impeller was conducted at this time. The test apparatus comprised a specimen, a specimen mount, a slurry jet nozzle, a tank with a water-cooling jacket for mixing water and solid particles, and a slurry transfer pump. The nozzle with an inner diameter of 3 mm was attached 25 mm away from the

Received September 1 2008; revised November 17 2008; accepted for publication November 15 2008: Review conducted by Prof. Tong Seop Kim. (Paper number O08025)
Corresponding author:Kenichi Sugiyama, sugiyama.kenichi@er.ebara.com

specimen surface in an opposing position. The nozzle produced a jet of slurry that impacted on and damaged the specimen surface. Each specimen was fixed in such a way that its surface was at 90 ° or 30 ° in relation to the slurry jet direction. The slurry flow velocity was set to 20 and 30 m/s. The tank was equipped with a water-cooling jacket to keep the slurry temperature between 20 and 35 °C. A mixture of tap water (80 L) and silica sand of 1 mass percent was used as slurry. The wear depth of each specimen was measured at predetermined intervals using a surface texture measuring instrument (Tokyo Seimitsu Co., Ltd.'s SURFCOM 1400D-3DF-12 with an accuracy of 0.01 μm).

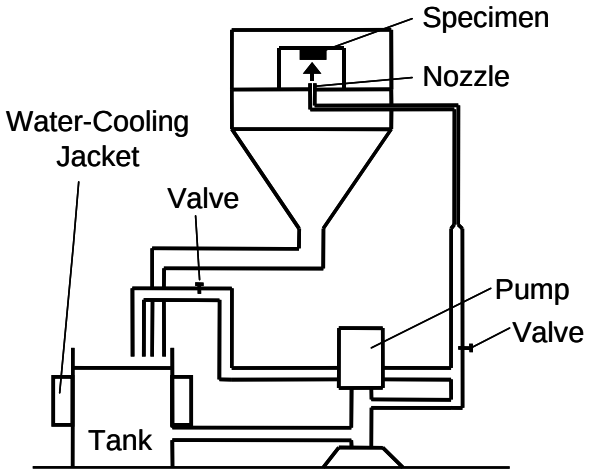

Fig. 1 Comparison of performance curves between optimum and reference blade shapes

Figure 2 shows the cross-sectional diagram of the pump used for the slurry wear test of the impeller. The pump comprised an impeller with an outer diameter of 255.17 mm, a diffuser vane, and a volute chamber, and the impeller has six blades. An impeller made of A5056 was used to assure wear of the impeller in a short time. The water temperature during operation was set at approximately 40 °C, the flow rate at 4.5 m^3/min, the rotating speed at 2500 rpm, the sand concentration at 1 mass%, and the operation time at 100 hours. The blade shape before and after the test was measured by a three-dimensional shape measurement system to calculate wear depth distribution.

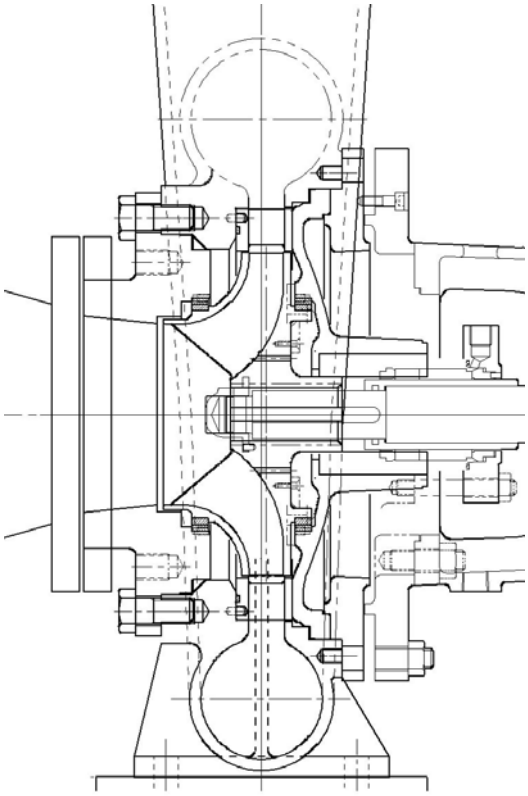

Fig. 2 Cross-sectional diagram of a pump for slurry wear test

Figure 3 shows the particle size distribution of silica sand for the test. Table 1 shows the chemical composition of silica sand. The mean diameters of the sand used for the slurry jet test and the impeller slurry wear test are 58 and 68 μm, respectively, at d50 (particle diameter corresponding to 50 % cumulative weight). The concentration of silica sand according to chemical components is 2300 kg/m^3.

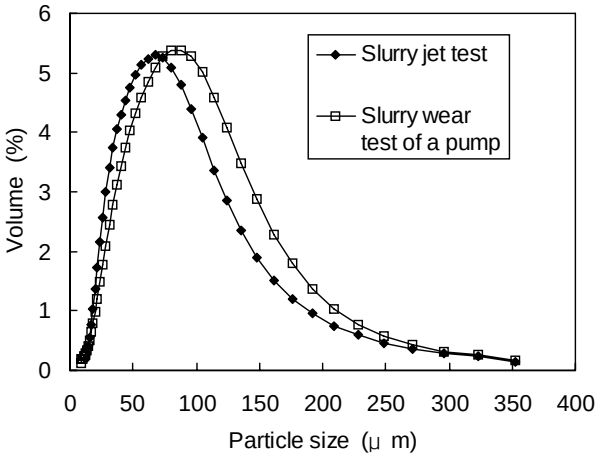

Fig. 3 Particle size distribution of silica sand

Table 1 Chemical composition of silica sand

SiO_2	90.2%
Al_2O_3	5.9%
Fe_2O_3	0.2%
$CaCO_3$	0.0%
Volatile total solids	0.0%
Total	96.3%

2.2 Analysis of particle behavior in the slurry jet test apparatus and the impeller slurry wear test apparatus

A part of this study has already been discussed in other papers [4], [5], but the outline is reviewed since the same method was again required for this study.

Based on stationary solutions obtained from single-phase (water) flow analysis using Star-CD, general-purpose flow simulation software, the behavior of individual particles was tracked with the Lagrange method. Analysis with the Lagrange method employed a model using a single-particle drag coefficient. The fluid drag force on particles was taken into account, but neither the particle drag force on the fluid nor the rotation of particles was considered. Due to low particle concentration, no interaction between particles was taken into account. For single-phase flow analysis, the standard k-ε model was used as a turbulent flow model.

An initial particle velocity of 20 or 30 m/s (the same velocity as that of the water) in the nozzle was provided to conduct the simulation for particle diameters of 10, 30, 50, 80, 120, 160, 200, and 300 μm. The number of times each particle impacted on the specimen surface was one; behavior analysis for the particle was stopped at the first impact. The particle density was set to 2300 kg/m^3 for this test.

Figures 4 and 5 show mesh divisions used for analysis at impact angles of 90 ° and 30 °, respectively. The analysis region for the test at an impact angle of 90 ° was axisymmetrically configured with the periodic boundary set at an angle of 60 °.

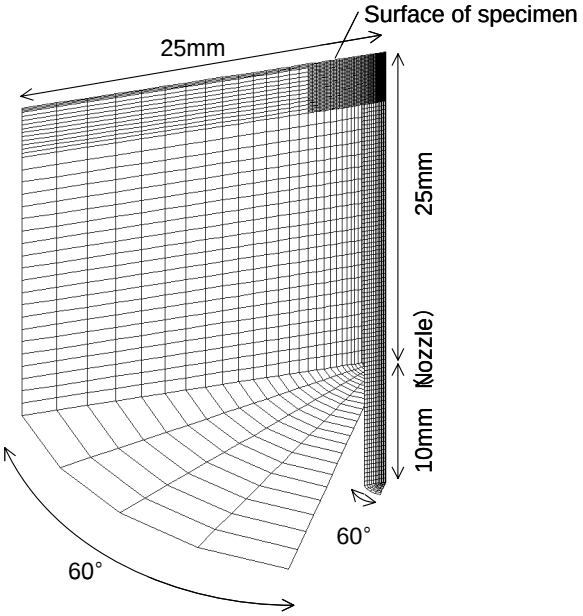

Fig. 4 Calculation model (impingement angle: 90 deg.)

The center of the nozzle outlet shape projected onto the specimen surface was defined as the specimen center. For analysis at an impact angle of 30 °, the impact position on the side of the specimen nearest the nozzle was indicated as a negative distance from the specimen center, while the impact position on the side farthest from the nozzle was indicated as a positive distance from the center.

Figure 6 shows mesh divisions of a flow channel and impeller only. The analysis was conducted only for the flow channel; the numbers of particles input for the analysis were 242,191.

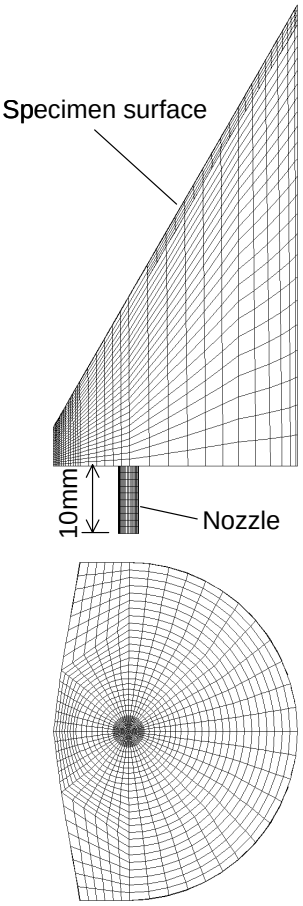

Fig. 5 Calculation model (impingement angle: 30 deg.)

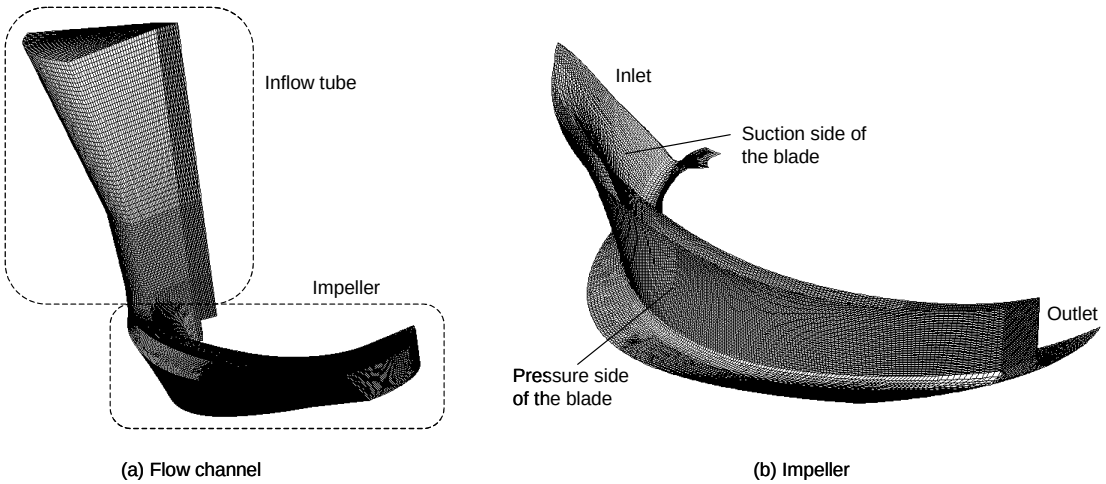

Fig. 6 Calculation model (inflow tube and impeller)

2.3 Derivation of an equation for wear depth prediction

In the same method as described in a previous paper [5], an equation for predicting slurry wear depth is derived from the results of the particle behavior analysis and the results of the slurry jet test.

According to a report by Bitter [6-7], the amount of wear volume loss is proportional to the kinetic energy of particles. Assuming the kinetic energy of solid particles as E (N· m), the wear rate $W(X)$ (mm/s) at the particle impact position X (mm) can be expressed as follows.

$$W(X) = C \times E = C \times \frac{1}{2} \times m \times V^2 \tag{1}$$

C, m, and V represent the constant, particle mass and particle velocity upon impact on the specimen surface. A wide distribution of slurry particle sizes makes it difficult to examine the dependency of slurry wear on the impact angle for each particle diameter. By setting the mean particle diameter as a reference particle size (D_0 = 60 μm) and the nozzle jet velocity as a reference velocity (V_0 = 20 m/s), the relation between the volume loss per particle Y (mm^3) and the impact angle α (deg.) is expressed by the following cubic function.

$$Y = a \cdot \alpha^3 + b \cdot \alpha^2 + c \cdot \alpha \tag{2}$$

The values of a, b, and c in the equation above are unknown. Using the cubic function is convenient for expressing both curves having peaks at a large impact angle and those having peaks at a small impact angle. Y is a material-specific value and corresponds to C in Eq. (1). The effect of the particle shape, which is difficult to formulate, has been ignored in the prediction equation. For establishing an equation for wear depth prediction, it is necessary to use particles with the same characteristics as those in actual environments.

Since the wear depth must be considered for each particle diameter, particle diameters are divided into 42 levels in a range between 10.09 and 352 μm. Considering the contribution of each particle, the wear rate W (X) at the impact position X is expressed as follows.

$$W(X) = \sum_{D=10.09}^{352} \left(a \cdot \alpha_{D,X}{}^3 + b \cdot \alpha_{D,X}{}^2 + c \cdot \alpha_{D,X} \right) \cdot (D/D_0)^3 \cdot (V_{D,X}/V_0)^2 \cdot F_{D,X} \tag{3}$$

(D = 10.09 to 352)

$\alpha_{D,X}$, D, $V_{D,X}$, and $F_{D,X}$ represent the impact angle (deg.), particle diameter (μm), Impact velocity (m/s), and impact frequency (1/(mm^2· s)). With non-dimensional values D_0 and V_0 of the particle mass and velocity, the particle density is removed from Eq. (3). The values of a, b, and c are determined by selecting three positions X on the wear surface after the slurry jet test and by formulating a simultaneous equation.

The positions X were selected so as to satisfy: 1) a position in which particles of all diameters impact and 2) a position in which particles impact at a wide range of impact angles from small to large angles. Thus, two positions 0.2 and 1.8 mm away from the specimen center were selected for the test at an impact angle of 90 ° and - 2.0 mm was selected for the test at an impact angle of 30 °.

According to a report by Wang [8], sand of a certain particle diameter or less has almost no contribution to the slurry wear of fluid machines. Assuming that "impacting particles with a certain level of kinetic energy or less does not cause material damage," the sum of kinetic energy of every particle per unit time and unit area supplied at test angle 90 ° and impact position 1.8 mm was calculated based on the analysis results, and the lower critical value of the kinetic energy was determined so that the ratio between the flow velocities 20 and 30 m/s corresponds to the ratio of the wear rate obtained from the test.

Solving the simultaneous equation provides the values of a, b, and c, by using the results of the test at a flow velocity of 20 m/s and by excluding particles having kinetic energy equal to or lower than the lower critical value obtained above from Eq. (3).

3. Test result and discussion

3.1 Results of the slurry jet test

Figure 7 shows the A5056 specimen's surface profile at a silica sand concentration of 1 %, an impact angle of 90 °, and a flow velocity of 20 m/s. The figure shows W-shaped curves [6], which are typically observed in the slurry jet test apparatus that

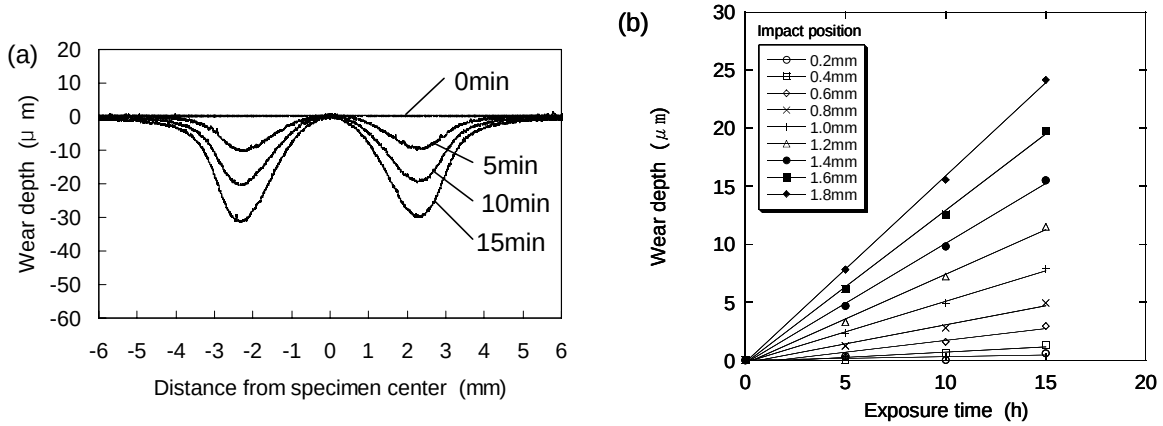

Fig. 7 Slurry jet test results for A5056, (a) surface profiles, (b) erosion curve at each impact position (flow velocity: 20m/s, silica sand: 1%, impingement angle: 90 deg.)

generate more intensive wear in the area surrounding the center of the jet flow than at the jet flow center. The position of the maximum wear depth moves gradually away from the specimen center with time. This fact suggests that particle behavior (trajectory) near the maximum wear depth position changes as the wear depth increases. Therefore, for wear depth evaluation, the region within the 1.8 mm position, where particle behavior is little affected, is selected. The wear depth at an impact position of 1.8 mm linearly increases in proportion to the exposure time. The results of specimen surface profile at a velocity of 30 m/s are omitted because they show the same tendency as in the case of 20 m/s.

Figure 8 shows the results of the test at an impact angle of 30°. This surface profile was made under the conditions of 1 % silica sand concentration, a 30° impact angle, and a flow velocity of 20 m/s. The maximum wear position is at - 2.5 mm. The wear depth at any impact position increases in proportion to the exposure time.

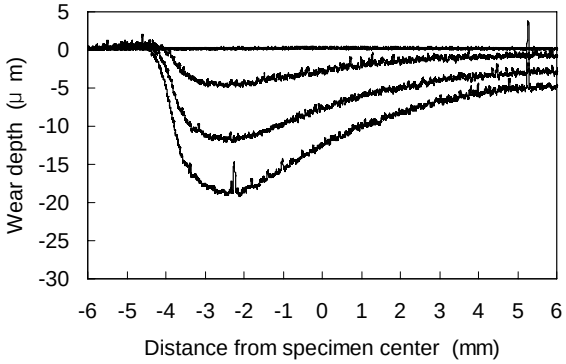

Fig. 8 Surface profiles for A5056 in slurry jet test
(flow velocity: 20m/s, silica sand: 1%, impingement angle: 30 deg.)

3.2 Results of particle behavior analysis using the slurry jet test apparatus and derivation of an equation for wear depth prediction

As an example of the result of particle behavior analysis, Figure 9 shows the relation between the impact position and the impact velocity and angle on the specimen surface in the case of an impact angle of 90° and a flow velocity of 20 m/s. The impact velocity is small near the specimen center and increases as the position moves toward the outside. In addition, the smaller the particle diameter, the lower the impact velocity at the same impact position. Though particles impact on the specimen at nearly 90° near the specimen center, the angle decreases toward the outside. Also, the smaller the particle diameter, the smaller the impact angle at the same impact position.

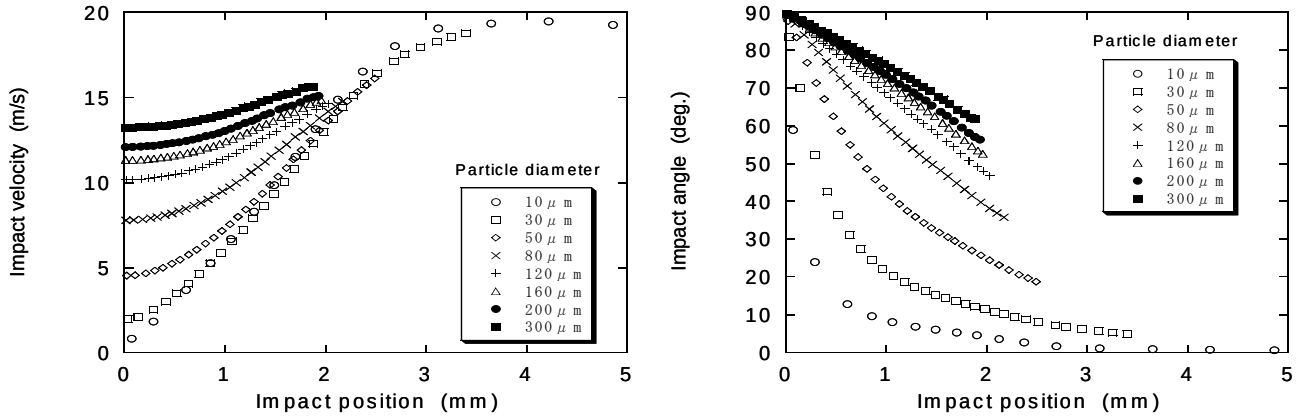

Fig. 9 Calculation results for slurry jet test (flow velocity: 20m/s, impingement angle: 90 deg.)

Figure 10 shows the distribution of kinetic energies of silica sand at flow velocities of 20 and 30 m/s, an impact angle of 90 °, and an impact position of 1.8 mm, as calculated from the particle behavior analysis. The x-axis represents the kinetic energy per particle, the left y-axis represents the particle diameter, and the right y-axis represents a value obtained by multiplying kinetic energy per particle by the impact frequency ($1/(mm^2 \cdot s)$). The sums of the kinetic energy (shaded part in the figure) of every particle having a kinetic energy of 7×10^{-8} or more are 3177 and 14863 ($N \cdot m/(mm^2 \cdot sec)$) with a ratio 1 to 4.7 at the flow velocities of 20 and 30 m/s, respectively. The wear rate in the wear test at the 1.8 mm impact position and at flow velocities of 20 and 30 m/s are 98 and 458 μm/h with a ratio of 1:4.7, which corresponds to the ratio in the sums of the kinetic energy mentioned above. Thus, the lower critical value of the kinetic energy is 7.0×10^{-8}.

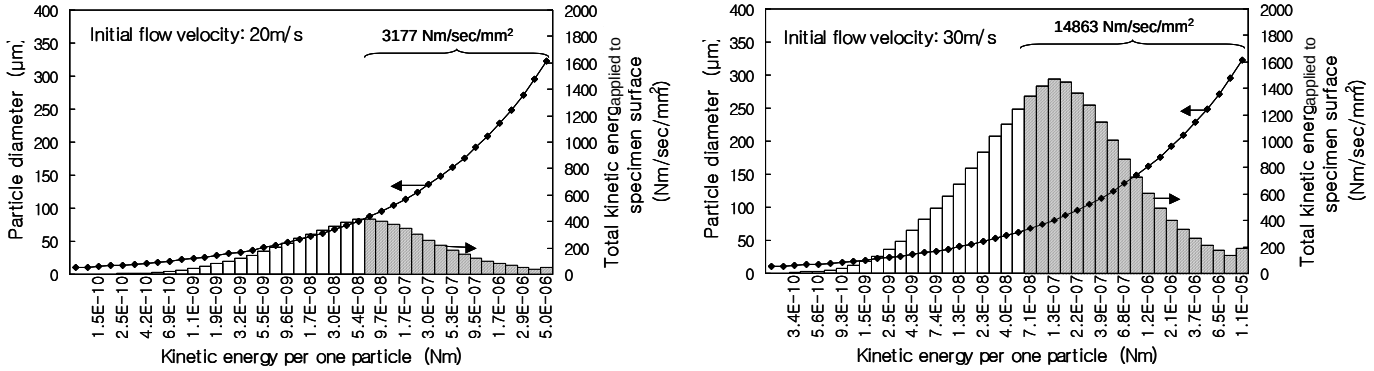

Fig. 10 Distribution of kinetic energy on impact particles (impact position: 1.8mm, silica sand: 1% , impingement angle: 90 deg.)

Figure 11 shows a graph plotted according to Eq. (2) based on the values of a, b, and c in Eq. (3). The values of a, b, and c are 2.69×10^{-15}, -6.19×10^{-13}, and 3.36×10^{-11}, respectively. This graph expresses the relation between the volume loss per particle and the impact angle with the reference particle diameter (60 μm) and at the reference velocity (20 m/s). The maximum volume loss is observed at an impact angle of approximately 35 °; this result agrees with the previous report [9], which says that the wear rate is at maximum at a smaller impact angle for ductile materials.

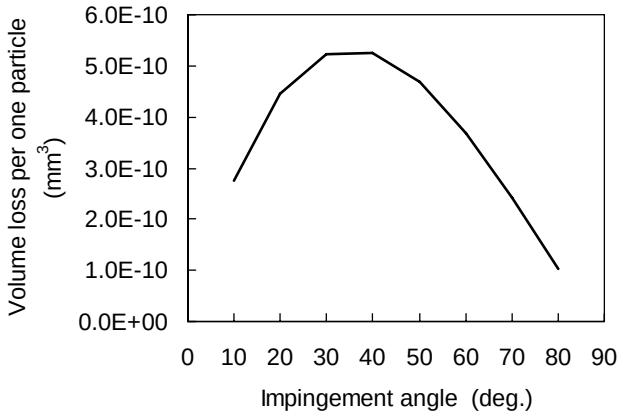

Fig. 11 Relation between impact angle and calculated volume loss for A5056 per one particle (particle diameter: 60 μ m, impact velocity: 20m/s)

3.3 Comparison of the result of the slurry wear test for the impeller to the prediction of wear depth distribution

Figure 12 shows the results from measuring the wear depth on the pressure and suction sides of the blade after the slurry wear test. The colored area in the figure indicates the section that can be measured with the three-dimensional shape measurement system. For easy recognition of wear depth distribution, the figure covers a wear depth of 0.0 to 1.4 mm with the maximum value indicated at the upper right. It reveals that the wear depth at the inlet on the pressure side and at the outlet on the suction side is large. Outside the section that can be measured with the three-dimensional shape measurement system, the area near the shroud at the inlet on the pressure side is severely worn with a wear depth of several millimeters at the edge. The area near the hub at the outlet on the suction side is also severely worn.

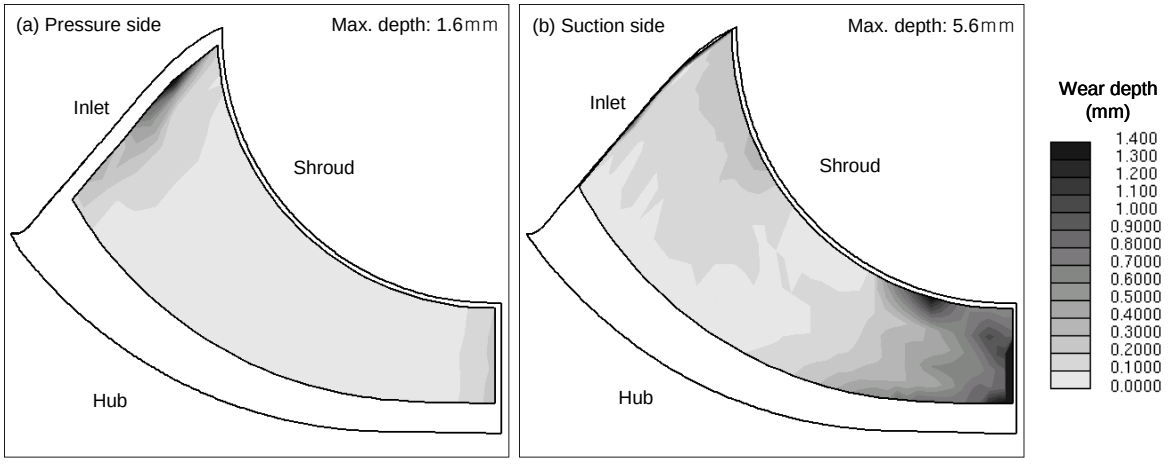

Fig. 12 Wear depth distribution for the A5056 blade after 100h slurry wear test

To exemplify the analysis of particle behavior for the blades, Figures 13 and 14 show the distributions of impact velocities and angles of 10, 120, and 300 μm particles on the pressure and suction sides. These figures show that, regardless of particle size, many particles impact on the inlet with an impact velocity of approximately 10 m/s and at a large impact angle of up to approximately 89°. There is a tendency for small particles to impact on the outlet on the pressure side with an impact velocity of up to approximately 26 m/s, which is close to the impeller periphery speed (33 m/s), and at a low impact angle of 10° or less. There is also a tendency for large particles to impact on the outlet on the suction side with an impact velocity of up to approximately 19 m/s and at a low impact angle of 10° or less. These findings suggest that significant wear observed at the outlet on the suction side after the test is attributable to the impact of large particles.

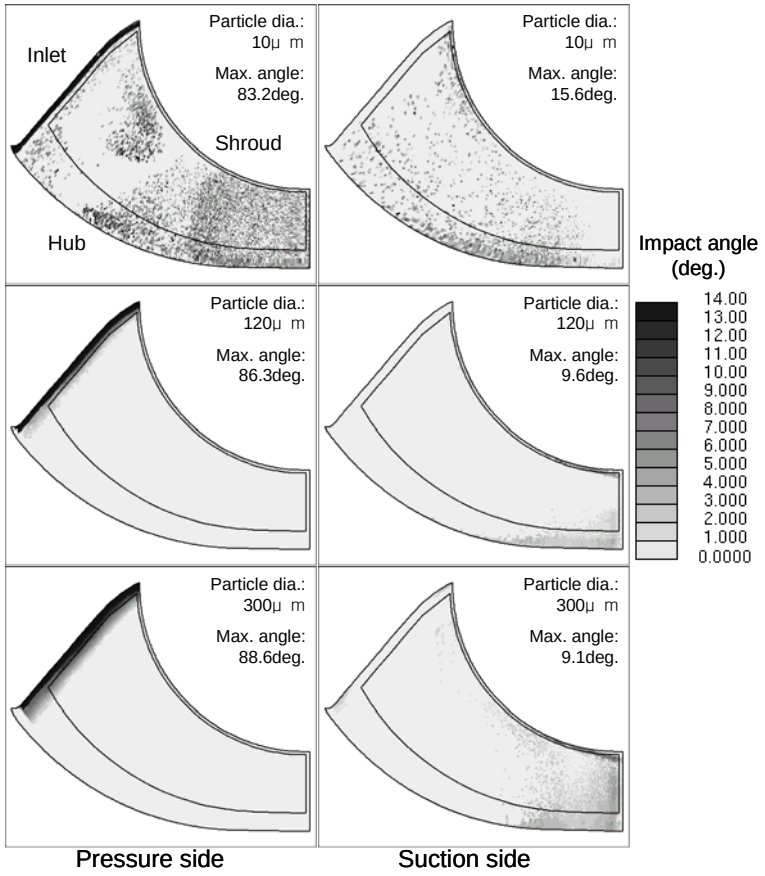

Fig. 13 Calculation results for the impact velocity of a particle on the blade

Figure 15 shows a wear depth distribution calculated by combining the results of particle behavior analysis and Eq. (3). The figure covers nine different particle diameters: 10, 30, 50, 80, 120, 160, 200, 240, and 300 μm. Figure 15 indicates a large wear depth at the inlet on the pressure side and at the outlet on the suction side, agreeing well with the results shown in Figure 12. The figure shows that the wear depth is large near the shroud at the inlet on the pressure side and near the hub at the outlet on the suction side, as is the case with Figure 12. These deeply worn areas almost correspond to the sections where a large wear depth was determined with the three-dimensional shape measurement system. At the same time, it is estimated that the particle behavior changes as the shape of the actual blade changes due to wear. Since the behavior change is more significant at the inlet with large wear depth, a wear depth of 54.4 mm, which is considerably larger than the measurement results, was predicted for the inlet on the pressure side (not covered by the measurement). The analysis predicted that the area with small wear depth observed after the test would suffer almost no wear because of extremely low particle impact frequency. This prediction result suggests that the number of particles input for the analysis was insufficient. Nonetheless, our prediction technique may be quite useful for industrial purposes in terms of prediction accuracy.

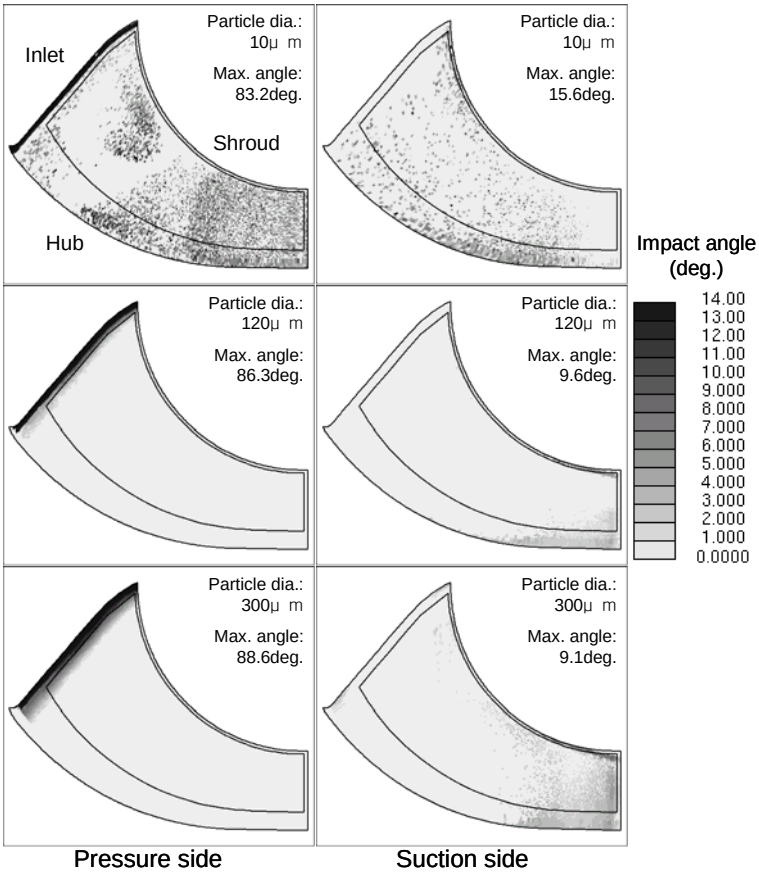

Fig. 14 Calculation results for the impact angle of a particle on the blade

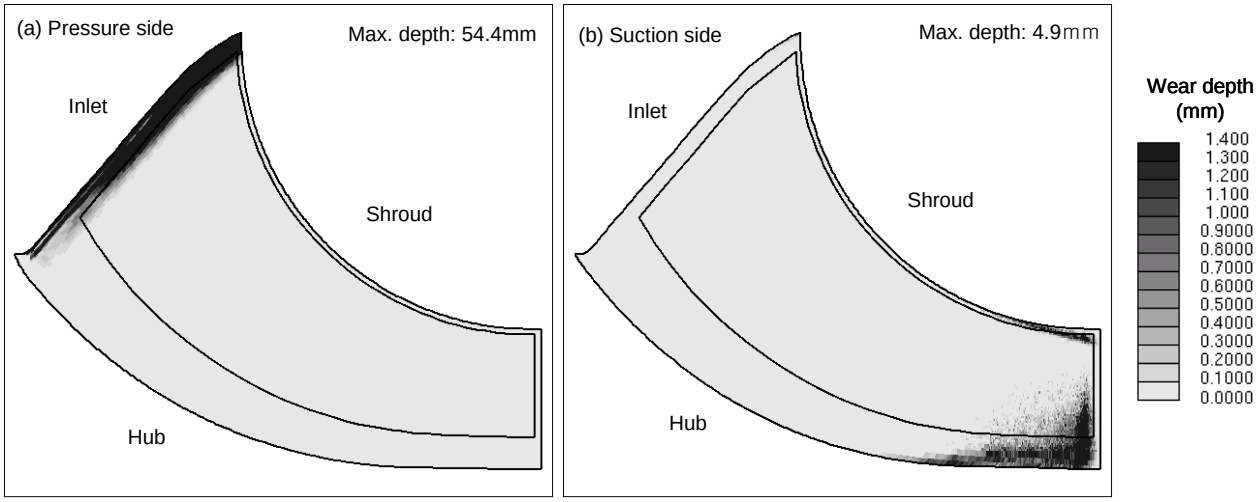

Fig. 15 Prediction results for the wear depth distribution of the aluminum blade after 100h slurry wear test

4. Conclusions

The distribution of slurry wear depth of an impeller made of A5056 was predicted by slurry jet test and particle behavior analysis. By comparing the results of the slurry wear test for the impeller to the prediction results, the following conclusions have been obtained.

(1) For slurry wear from silica sand used in the test, the maximum wear volume of the A5056 material is obtained at a particle impact angle of around 35 °, and the lower critical value of the kinetic energy of particles is approximately 7 x 10^{-8} N· m.

(2) The impeller in this study is deeply worn at the inlet on the pressure side and at the outlet on the suction side because many large particles impact there.

(3) The predicted wear depth at inlet on the blade is larger than measurement results after test. It is estimated the particles behavior changes due to large wear.

(4) The comparison of the results of particle behavior analysis for the impeller to the results of the wear test shows a correlation between the impact position of particles determined by the analysis and the wear depth distribution obtained by the test. In terms of quantitative prediction accuracy for wear depth distribution, our prediction technique may be quite useful for industrial purposes.

Nomenclature

C	Constant	V	Particle velocity [m/s]
D	Particle diameter [μm]	V_0	Nozzle jet velocity as a reference velocity [μm]
D_0	Particle diameter as a reference particle size [μm]	W	Wear rate [mm/s]
E	Kinetic energy [Nm]	X	Particle impact position [mm]
F	Impact frequency[1/(mm^2・s]	Y	Volume loss per particle [mm^3]
m	Particle mass [kg]	α	Impact angle [degree]

References

[1] Oka, Y., Matsumura, M., Yamawaki, M., and Sakai, M., "Jet-in-silt and Vibratory Methods for Slurry Erosion-Corrosion Tests of Materials," 1987, ASTM STP946, pp. 141-154.

[2] Hattori, S., Maekawa, N., Miura, T., Hirafuji, T., and Okada, T., "Evaluation of Slurry-Wear Resistance of Pump Materials and its Application to Prototype Tests," 1996, Transactions of the Japan Society of Mechanical Engineers. A, 62, 593, pp. 74-81.

[3] Nomoto, S., Tani, K., and Shimmei, K., "Evaluation of Silt Abrasion for Hydraulic Machinery Using Numerical Flow Analysis," 2006 23rd IAHR Symposium - Yokohama.

[4] Hattori, S., Harada, K., and Sugiyama, K., "Convenient Prediction Method of Impingement Angle Dependence of Slurry Wear," 2005, Turbomachinery, 33, 7, pp. 443-451.

[5] Sugiyama, K., Harada, K., and Hattori, S., "Prediction of the Volume Loss by Using Slurry Jet Test on SCS6," 2006,Transactions of the Japan Society of Mechanical Engineers. A, 72, 722, pp. 1569-1576.

[6) Bitter, J. G. A., "A Study of Erosion Phenomena, Part 2," 1963, Wear, 6, pp. 169-190.

[7] Editing committee of “Erosion/Corrosion and the application technology”, “Erosion/Corrosion and the application technology,” 1987, pp. 39, Industrial Publishing & Consulting, Inc.

[8] Wang, Z., W., "Current Situation and Progress in the Protecting Measures for Hydraulic Turbine Abrasion-Cavitatin in China," 2003, ABRASION AND CAVITATION IN HYDRAULIC MACHINERY, pp. 19-24.

[9] Kiselev, G. J., "Wear Resistance of Metals Subjected to an Abrasive Hydraulic Medium," 1971, Russian Engineering Journal, 51, 12, pp. 10-12.